Int J Ind Chem (2014) 5:14
DOI 10.1007/s40090-014-0014-8

RESEARCH

# Fischer–Tropsch synthesis on cobalt–manganese nanocatalyst: studies on rate equations and operation conditions

**Mohsen Mansouri · Hossein Atashi · Farshad Farshchi Tabrizi · Ghobad Mansouri · Naimeh Setareshenas**

Received: 22 January 2013 / Accepted: 31 March 2014 / Published online: 8 May 2014


**Abstract** In this research, an active Co–Mn/$TiO_2$ catalyst was prepared by co-precipitation method for synthesis of light olefins in Fischer–Tropsch synthesis. After studying the effects of using optimized operating conditions on catalyst performance, the kinetic of experimental study was performed in a differential fixed-bed micro reactor. The effect of a range of operating variables such as the pressure, temperature, and $H_2$/CO molar feed ratio on the catalytic performance of precipitated catalyst were investigated. It was found that the best operating conditions are $H_2$/CO = 2/1, $T$ = 270 °C, and $P$ = 3 bar. Power-law equations have been fitted with experimental data in terms of the hydrogen and carbon monoxide partial pressure for the CO conversion rate and production rates for each product. The activation energies for the carbon monoxide conversion and methane production were determined to be 30.71 and 42.37 kJ/mol, respectively.

M. Mansouri (✉) · H. Atashi · F. F. Tabrizi · N. Setareshenas
Department of Chemical Engineering, University of Sistan and Baluchestan, 98164-161 Zahedan, Iran
e-mail: mansouri@pgs.usb.ac.ir

H. Atashi
e-mail: atashi.usb@gmail.com

F. F. Tabrizi
e-mail: farshchi@eng.usb.ac.ir

N. Setareshenas
e-mail: setareshenas@pgs.usb.ac.ir

F. F. Tabrizi
Department of Chemical Engineering, School of Chemical and Petroleum Engineering, Shiraz University, Shiraz, Iran

G. Mansouri
Department of Chemistry, Payame Noor University, 19395-3697 Tehran, Iran
e-mail: mansouri.gh@gmail.com

**Keywords** Fischer–Tropsch synthesis · Fixed-bed reactor · Power-law equation · Operation conditions

**List of symbols**

| | |
|---|---|
| $L_b$ | Length of catalytic bed (m) |
| $d_p$ | Particle diameter (m) |
| $F$ | Molar flow rate (mol/min) |
| $T$ | Temperature (°C) in kinetic equation (K) |
| $R$ | Universal gas constant (8.314 J/mol. K) |
| $P_{H_2}$ | Partial pressure of hydrogen (atm) in kinetic equation (bar) |
| $P_{CO}$ | Partial pressure of carbon monoxide (atm) in kinetic equation (bar) |
| $R^2$ | Goodness of fit |
| $W$ | The catalyst weight (g) |

## Introduction

Fischer–Tropsch synthesis (FTS) has received renewed interests in recent years because of the global demand for a decreased dependence on petroleum for production of fuels and chemicals. FTS is a heterogeneous catalytic process for the transformation of synthesis gas (syngas, CO + $H_2$) into hydrocarbons [1, 2]. This process was first reported more than 80 years ago by two German chemists, Fischer and Tropsch [3]. The FT process generally includes the following reactions [4]:

$$\text{Paraffin formation: } (2n+1)\ H_2 + nCO \rightarrow C_nH_{2n+2} + nH_2O \quad (1)$$

$$\text{Olefin formation: } 2nH_2 + nCO \rightarrow C_nH_{2n} + nH_2O. \quad (2)$$

In some references, these equations have been summarized in an alternative way [5]:

$$(1 + m/2n)\ H_2 + \ CO \ \rightarrow \ (1/n)\ C_nH_m + \ H_2O, \qquad (3)$$

where $n$ refers to the length of the carbon chain and m is the average number of hydrogen atoms in the hydrocarbon molecule. Chemicals such as a-alkenes may also be directly produced from syngas if a highly selective FT catalyst can be developed.

The typical active metals used in FT catalysts are Fe, Co, and Ru although several other metals, such as Ni and Rh, also exhibit activities for Eqs. (1–3) [6]. Both cobalt and iron have been employed in industry for FTS. Fe is cheaper than Co, but Co-based catalysts are generally more active and more selective to linear long-chain hydrocarbons. Moreover, Co catalysts are typically more resistant to deactivation by water [7, 8]. Thus, Co catalysts have attracted much attention for the synthesis of long-chain linear hydrocarbons, such as wax and diesel fuel [7, 9].

However, very wide product distributions are generally obtained over conventional FT catalysts. Selectivity control remains one of the most important and difficult challenges in the research area of FTS. Generally, the nature of the catalyst, the reactor, and the operating conditions are the main factors affecting the product selectivity and the CO conversion activity for FTS. $TiO_2$ supported catalysts have been shown to have a strong metal–support interaction [10] which makes the cobalt species difficult to be reduced, most likely due to a strong Co–O interaction with the support that are reduced only at very high temperatures [11]. It was shown that the addition of Mn to Fe or Co catalysts brought about a significant increase in high olefin formation and a decrease in methane activity [12, 13]. Co–Mn catalysts have been investigated intensively for their higher selectivity to produce $C_2$–$C_3$ olefins [14]. Recently efforts have also been done to optimize the Co content in the bulk precipitated catalysts [15], to understand the effect of cobalt on activities of the bifunctional catalysts and also to find the optimum conditions for the production of $C_2$–$C_4$ olefins in maximum amounts [16].

The kinetic description of the FT reaction is a very important task for industrial practice, being a prerequisite for the industrial process design, optimization, and simulation. The kinetics of cobalt-based FT catalysts has been a subject of research for decades. The mechanistic kinetic rate expressions for cobalt catalysts are based on the formation of the monomer species as the rate-determining step in the consumption of synthesis gas. Many kinetic equations have been proposed in the literature for various cobalt catalysts, and these have been obtained either empirically (using a power-law rate equation) or to fit a proposed mechanism [17–23]. A few power-law rate equations over various cobalt catalysts are presented in Table 1 [19–23].

The objective of this work is to determine the reaction rates and selectivity of products for FTS on a titania-supported cobalt–manganese nanocatalyst, which was prepared by co-precipitation method. After studying the effects of using optimized operating conditions on catalyst performance, the kinetic of experimental study was carried out over a wide range of reaction conditions. A few experiments have been carried out in a fixed-bed differential reactor under nearly isothermal conditions. Based on the experiments, a number of power-law rate equations have been presented. The appropriate models were obtained and the kinetic parameters were determined.

## Methods

### Materials and processing

Co–Mn catalysts (25 %Co/75 %Mn/30 wt.% $TiO_2$) tested in this study were prepared using co-precipitated procedure which is described elsewhere [2]. Aqueous solutions of $Co(NO_3)_3{\cdot}6H_2O$ (0.5 M) (99 %, Merck) and $Mn(NO_3)_2{\cdot}4H_2O$ (0.5 M) (99 %, Merck) with different molar ratios were pre-mixed and the resulting solutions were heated to 70 °C in a round bottomed flask fitted with a condenser. Aqueous $Na_2CO_3$ (0.5 M) (99.8 %, Merck) was added to the mixed nitrate solution in a dropwise manner with stirring while the temperature was maintained at 70 °C until pH 8 ± 0.1 was achieved. The resulting precipitate was then left in this medium for times ranging 0–240 min. The aged precipitate was then filtered and washed several times with warm distilled water. The precipitate was then dried in the an oven (120 °C, 16 h) to give a material denoted as the catalyst precursor, which was subsequently calcined in static air in a furnace (500 °C, 16 h) to give the final catalyst. Then, to prepare $TiO_2$ supported catalyst, the amount of 30 wt.% of $TiO_2$ based on the total catalyst weight was added to the mixed solution of cobalt and manganese nitrates with the molar ratio of 25 %Co/75 % Mn and then filtered, washed, dried at 120 °C, and calcined at 500 °C for 16 h, in the same way as for the unsupported catalyst preparation. The catalyst sample was also characterized by X-ray diffraction, scanning electron microscopy and Brunauer–Emmett–Teller (BET) surface area methods, as demonstrated in our previous work [2].

The BET specific surface area of precursor was found to be 138.2 $m^2/g$. The BET specific surface area resulting from the calcined catalysts (before and after FTS) is given in Table 2. According to this table, it can be observed that the surface area values obtained for the calcined catalyst

**Table 1** Summary of kinetic studies based on power law rate of the FTS on cobalt catalysts

| References | Catalyst | Reactor type | $T$ (°C) | $P$ (bar) | $H_2/CO$ | $-r_{CO}$[a] |
|---|---|---|---|---|---|---|
| [19] | $Co/TiO_2$ | FBR | 200 | 8–16 | 1–4 | $k P_{CO}^{-0.24} P_{H_2}^{0.74}$ |
| [20] | $Co/B/Al_2O_3$ | FBR | 170–195 | 1–2 | 0.25–4 | $k P_{CO}^{-0.5} P_{H_2}^{0.68}$ |
| [21] | $Co/La_2O_3/Al_2O_3$ | Berty | 215 | 5.2–8.4 | 2 | $k P_{CO}^{-0.33} P_{H_2}^{0.55}$ |
| [22] | $Co/CuO/Al_2O_3$ | FBR | 235–270 | 1.7–55 | 1–3 | $k P_{CO}^{-0.5} P_{H_2}$ |
| [23] | $Co/MgO/ThO_2$/kieselguhr | FBR | 185–200 | 1 | 2 | $k P_{CO}^{-1} P_{H_2}^{2}$ |

*FBR* fixed-bed reactor

[a] $k$ is temperature-dependent constants

**Table 2** BET surface area ($m^2/g$) result for both precursor and calcined catalysts containing 25 %Co/75 %Mn/30 wt.% $TiO_2$ [2]

| Precursor | Calcined catalyst (before FTS) | Calcined catalyst (after FTS) |
|---|---|---|
| 138.2 | 136.8 | 135.2 |

(before FTS) are relatively higher than that observed for the tested catalyst.

The average value of the crystal size in the $Co–Mn/TiO_2$ nanocatalyst was determined to be about 21 nm by using Scherrer equation. A temperature-programmed reduction determination showed reduction peaks at 225, 320, and 460 °C. Using the definition of "degree of reduction" (DR), the value of DR for $Co–Mn/TiO_2$ catalyst was 89 %.

## Catalytic test

The experiments were carried out in a fixed-bed tubular stainless steel micro reactor. A schematic representation of the experimental set up is shown in Fig. 1 [2]. All gas lines to the reactor bed were made from 1/4″ stainless steel tubing Three mass flow controllers (Brooks, Model 5850E) were used to adjust automatically flow rate of the inlet gases comprising CO, $H_2$, and $N_2$ (purity of 99.99 %). The mixed gases in the mixing chamber passed into the reactor tube, which was placed inside a tubular furnace (Atbin, Model ATU 150-15) capable of producing temperature up to 1,500 °C and controlled by a digital programmable controller (DPC). The reactor tube was constructed from stainless steel tubing; internal diameter of 20 mm, with the catalyst bed situated in the middle of the reactor. The reaction temperature was controlled by a thermocouple inserted into catalyst bed and visually monitored by a computer equipped with software. Some thermocouples were inserted in the catalyst bed for monitoring the inlet, outlet, and bed temperatures by a DPC. Prior to the catalytic activity measurements, the samples were crushed, sieved (mesh size 0.1–2.5 mm), and then held in middle of the reactor using quartz and asbestos. The catalyst was in situ pre-reduced at atmospheric pressure under $H_2–N_2$ flow $H_2/N_2 = 1$ (flow rate of each gas = 30 ml/min) at 400 °C for 16 h before synthesis gas exposure. It consists of an electronic back pressure regulator which is able to control the total pressure of the desired process by remote control using TESCOM software package designed. This promotes the yield in the range of 1–100 bar. In each test, 1.0 g catalyst was loaded and the reactor operated about 12 h to ensure steady-state operations were attained. Reactant and product streams were analyzed on-line using a gas chromatograph (Thermo ONIX UNICAM PROGC +) equipped with sample loop, two thermal conductivity detectors (TCD) and one flame ionization detector (FID) able to perform the analysis of a wide variety of gaseous hydrocarbon mixtures, one TCD used for the analysis of hydrogen and the other one used for all the permanent gases such as $N_2$, $O_2$, and CO. The FID is used for the analysis of hydrocarbons. The system is applicable to the analysis of non-condensable gases, methane through $C_8$ hydrocarbons. The contents of the sample loop were injected automatically into an alumina capillary column (30 m × 0.550 mm). Helium was employed as a carrier gas for optimum sensitivity (flow rate = 30 ml/min). The calibration was carried out using various calibration mixtures and pure compounds obtained from Tarkib Gas Alvand Company (Iran).

Experiments were carried out with mixtures of $H_2$, CO, and $N_2$ in a temperature range of 190–270 °C, $H_2/CO$ feed ratio of 1/1–3/1 and a pressure range of 1–10 bar. The experimental conditions and obtained data are presented in Table 3. In all of the experiments, the space velocities were between 2,700 and 5,200 $h^{-1}$. To achieve the isothermal conditions in a catalytic bed, the catalyst was diluted with inert materials (quartz and asbestos) and axial temperature distribution was ensured using Mear's criterion [24, 25]. In order to avoid channelization, the following simplified relation between catalyst bed length ($L_b$) and mean catalyst particle diameter ($d_p$) was fulfilled, $L_b/d_p > 50$. We have a differential flow reactor when we choose to consider the rate to be constant at all points within the reactor. Since rates are concentration-dependent, this assumption is usually reasonable only for small conversions or for shallow small reactors. For each run in a differential reactor, the plug flow performance equation becomes as follows:

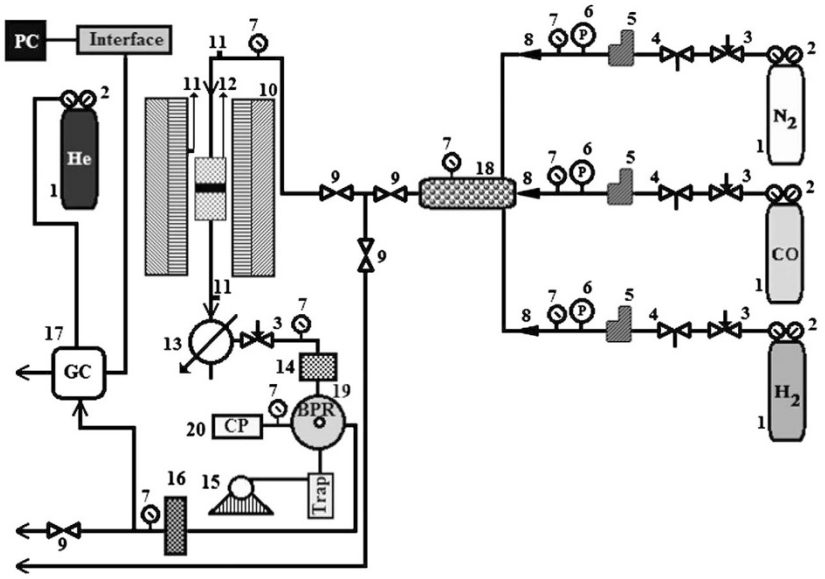


**Fig. 1** Schematic representation of the reactor used. *1* Gas cylinders, *2* pressure regulators, *3* needle valves, *4* valves, *5* mass flow controllers (MFC), *6* digital pressure controllers, *7* pressure gauges, *8* non return valves, *9* ball valves, *10* tubular furnace, *11* temperature indicators, *12* tubular reactor and catalyst bed, *13* condenser, *14* trap, *15* air pump, *16* silica gel column, *17* gas chromatograph (GC), *18* mixing chamber, *19* back pressure regulator (BPR, electronically type), and *20* control panel (CP)

**Table 3** Summary of experimental conditions for CO consumption and production rates of hydrocarbons at $P_{tot} = 1$–10 bar and $T = 190$–270 °C

| Run no. | $T$ (°C) | CO conv. (%) | $P$ (atm) | | $F/W$ (mol grcat.$^{-1}$ min) | Rate (mmol grcat.$^{-1}$ min) | | | |
|---|---|---|---|---|---|---|---|---|---|
| | | | CO | $H_2$ | | CO | CH4 | $C_3H_6$ | C5+ |
| 1 | 190 | 11.2 | 0.691 | 2.241 | 0.0019 | 0.218 | 0.023 | 0.054 | 6.464 |
| 2 | 190 | 11.1 | 1.154 | 3.533 | 0.0032 | 0.36 | 0.036 | 0.087 | 11.846 |
| 3 | 190 | 10.6 | 1.625 | 3.636 | 0.0045 | 0.481 | 0.045 | 0.115 | 16.469 |
| 4 | 200 | 11.9 | 0.686 | 1.466 | 0.0019 | 0.226 | 0.023 | 0.051 | 6.435 |
| 5 | 200 | 10.7 | 1.159 | 2.597 | 0.0031 | 0.339 | 0.032 | 0.078 | 10.572 |
| 6 | 200 | 9.2 | 2.122 | 4.675 | 0.0057 | 0.526 | 0.044 | 0.12 | 18.204 |
| 7 | 210 | 14.6 | 0.665 | 1.559 | 0.0018 | 0.272 | 0.0214 | 0.08 | 6.207 |
| 8 | 210 | 15.6 | 1.534 | 3.033 | 0.0043 | 0.679 | 0.038 | 0.194 | 17.626 |
| 9 | 210 | 14.3 | 2.225 | 5.2001 | 0.0062 | 0.889 | 0.044 | 0.244 | 23.772 |
| 10 | 220 | 15.6 | 0.657 | 1.559 | 0.0018 | 0.285 | 0.0176 | 0.064 | 6.901 |
| 11 | 220 | 14.9 | 1.988 | 4.675 | 0.0054 | 0.817 | 0.036 | 0.213 | 23.899 |
| 12 | 220 | 14.1 | 2.23 | 5.2001 | 0.0061 | 0.859 | 0.039 | 0.239 | 20.510 |
| 13 | 230 | 15.61 | 1.098 | 2.597 | 0.003 | 0.469 | 0.038 | 0.115 | 7.471 |
| 14 | 230 | 15.9 | 1.538 | 3.636 | 0.0042 | 0.657 | 0.063 | 0.162 | 13.644 |
| 15 | 240 | 18.6 | 1.762 | 4.675 | 0.0051 | 1.272 | 0.121 | 0.383 | 35.055 |
| 16 | 240 | 18.7 | 1.955 | 5.2005 | 0.0057 | 1.419 | 0.123 | 0.429 | 47.172 |
| 17 | 250 | 19.1 | 0.629 | 1.559 | 0.0017 | 0.329 | 0.038 | 0.1 | 6.997 |
| 18 | 250 | 20.3 | 1.035 | 2.597 | 0.0028 | 0.583 | 0.075 | 0.16 | 14.323 |
| 19 | 250 | 20.8 | 1.439 | 3.636 | 0.004 | 0.836 | 0.109 | 0.246 | 25.114 |
| 20 | 260 | 21.5 | 0.611 | 1.559 | 0.0017 | 0.363 | 0.067 | 0.099 | 6.901 |
| 21 | 260 | 23.2 | 1.701 | 4.675 | 0.051 | 1.380 | 0.179 | 0.401 | 41.375 |
| 22 | 270 | 22.8 | 0.194 | 0.559 | 0.0006 | 0.264 | 0.024 | 0.117 | 1.145 |
| 23 | 270 | 23.7 | 0.594 | 1.559 | 0.0016 | 0.393 | 0.067 | 0.181 | 8.141 |

$$\frac{W}{F_{CO}^{0}} = \int_{x_{in}}^{x_{out}} \frac{dx}{-r_{CO}} = \frac{-1}{r_{CO}} \int_{x_{in}}^{x_{out}} dx = \frac{x_{out} - x_{in}}{-r_{CO}} = \frac{x_{out}}{-r_{CO}}. \quad (4)$$

According to the above equation, the average rate for each run is derived as follows:

$$-r_{CO} = \frac{F_{CO}^{0} x_{out}}{W}. \quad (5)$$

The selectivity (%) towards the components on carbon-basis was calculated according to

$$\text{Selectivity of product } i\ (\%) = \frac{\text{moles of product } i}{\text{moles CO in} - \text{moles CO out}} \times 100. \quad (6)$$

The production rate for each product was [26]

$$r_i = n_{i,0}/W, \quad (7)$$

where $n_{i,0}$ and $W$ are molar flow rate of component $i$ exiting the reactor and the catalyst weight, respectively.

## Results and discussion

### Effect of operational conditions

Operational conditions are very important factors on the catalytic performance of the catalysts for FTS. Conventional FT catalyst screening consists of comparing the catalytic performance at the same experimental conditions (temperature, pressure, $H_2$/CO ratio, and amount of catalyst or active phase). The measured output values of catalyst screening are typically overall activity (syngas conversion), selectivities (methane, light, and heavy hydrocarbons), stability, and catalyst behavior during the start-up activation steps. The choice of the operating conditions and reactor represents the major challenge of FT catalyst screening. The effect of a range of operation variables such as $H_2$/CO feed molar ratios, reaction temperature, and reaction pressure on the catalytic performance of $TiO_2$ supported Co–Mn catalyst was investigated to identify and optimize the operational conditions for FTS. The typical reaction results are compared with respect to activity (CO conversion), product selectivity, and the formation of methane.

### Effect of temperature on product selectivity

The effect of reaction temperature on the catalytic performance of the 25 %Co/75 %Mn/30 wt.% $TiO_2$ prepared using co-precipitated procedure was studied at a range of temperatures between 190 and 270 °C under the same reaction conditions of $H_2$/CO = 2/1, gas hourly space velocity (GHSV) = 4,500 $h^{-1}$ at constant pressure 3 bar. The reduced catalyst was tested at each reaction temperature for 12 h and the results are shown in Table 4. According to the obtained results (Table 4), the optimum reaction temperature was 270 °C, at which temperature the total selectivity of light olefin products was higher than those at the other reaction temperatures under the same operating conditions. Because the FT polymerization reaction is exothermic, an increase in reaction temperature always shifts the product towards lower carbon number hydrocarbons [27]. Hence, 270 °C is considered to be the optimum operating temperature because of high CO conversion, high total selectivity of produced light olefins and low $CH_4$. In general, an increase in the reaction temperature leads to an increase in the catalytic performance; however, it was also shown that the reaction temperature should not be too low, since at low reaction temperatures the conversion percentage of CO is low [13]; Fernandes [28] reported that the lower temperatures than 180 °C may not provide enough energy to active the reagents on the catalyst, and the reaction may not begin. At high temperature the selectivities of $CH_4$ and $CO_2$ (as unwanted products) were enhanced, as well as the formation of large amount of coke (another unwanted product) [29]. On the other hand, lower temperature is preferential for chain growth and the production of heavy hydrocarbons [30].

**Table 4** The effect of temperature on the catalytic performance: $P$ = 3 bar; $H_2$:CO ratio (2:1)

| $T$ (°C) | CO conversion (%) | Selectivity (%) | | | |
|---|---|---|---|---|---|
| | | $CH_4$ | $C_2H_4$ | $C_3H_6$ | $C_{5+}$ |
| 190 | 11.2 | 16.5 | 20.9 | 22.8 | 27.6 |
| 210 | 14.6 | 14.8 | 22.4 | 27.5 | 20.8 |
| 230 | 16.6 | 15 | 23.3 | 20.5 | 22.2 |
| 250 | 19.1 | 17.7 | 23.1 | 28.4 | 20.7 |
| 270 | 23.7 | 15.6 | 32.9 | 27.8 | 16.8 |

### Effect of pressure on product selectivity

The total syngas pressure is an important catalyst screening parameter. Variation of pressure is also applied in directing the FT process toward desired products. The results of FT catalyst screening at atmospheric and high pressure could yield different results. These differences could be interpreted in terms of different concentrations of reagents in gaseous and liquid phases, catalyst restructuring, and deactivation. An increase in total pressure would generally result in condensation of hydrocarbons, which are normally in the gaseous state at atmospheric pressure. Higher pressures and higher carbon monoxide conversions would

**Table 5** The effect of pressure on the catalytic performance: $T = 270$ °C; $H_2$:CO ratio (2:1)

| $P$ (bar) | CO conversion (%) | Selectivity (%) | | | |
|---|---|---|---|---|---|
| | | $CH_4$ | $C_2H_4$ | $C_3H_6$ | $C_{5+}$ |
| 1 | 22.8 | 14.8 | 30.2 | 20.9 | 14.4 |
| 3 | 23.7 | 15.6 | 32.9 | 27.8 | 16.8 |
| 5 | 23.5 | 16.6 | 28.1 | 26.7 | 20.3 |
| 7 | 23.1 | 16.6 | 24.7 | 27.3 | 24.4 |
| 9 | 23.6 | 15.8 | 24.8 | 25.5 | 26.9 |
| 10 | 23.2 | 15.6 | 24 | 23.7 | 29.3 |

probably lead to saturation of catalyst pores by liquid reaction products [31]. Malek Abbaslou et al. [32] reported that as the pressure increases, the supercritical media exhibits a liquid-like density, which can enhance extraction from the catalyst pores. This phenomenon helps CO and $H_2$ adsorption onto active sites thereby increasing CO conversion. A different composition of the liquid phase in catalyst pores at high synthesis gas pressures could affect the rate of elementary steps and carbon monoxide and hydrocarbon concentrations. A series of experiments were carried out to investigate the influence of the reaction pressure on the catalytic performance of the cobalt manganese oxide catalyst containing 25 %Co/75 %Mn/30 wt.% $TiO_2$ for production of light olefins at the reaction conditions of $H_2/CO = 2/1$, GHSV = 4,500 $h^{-1}$ and 270 °C, during variation of total pressure in the range of 3–10 bar the reduced catalyst was tested at each pressure for 12 h. It can be seen from Table 5 that at the ranges of 1–10 bar total pressure, no significant change on CO conversion was observed. However, light olefins selectivities were changed and the results indicate that at the total pressure of 3 bar, the catalyst shows the highest total selectivity of 60.6 % with respect to $C_2$–$C_3$ light olefins. It is worth mentioning that at some experimental conditions only trace quantities of ethane, propane, butane, and $CO_2$ were observed which were negligible in comparison with light olefins. Hence because of higher total selectivity toward $C_2$–$C_3$ light olefins, a high value of CO conversion, and low $CH_4$ selectivity at the total pressure of 3 bar, this pressure was chosen as the optimum pressure.

## Effect of $H_2$/CO molar feed ratio on product selectivity

It is well known that H and CO coverage play essential roles in the reactivity and selectivity of FTS. The influence of the reaction $H_2$/CO molar feed ratio on the steady-state catalytic performance of the cobalt manganese oxide catalyst containing 25 %Co/75 %Mn/30 wt.% $TiO_2$ prepared using co-precipitation technique for the Fischer–Tropsch reaction at 270 °C under constant pressure of 3 bar was investigated. The results (not shown here) indicated that CO conversion increases with the increase of the $H_2$/CO molar feed ratios from 1/1 to 2/1, and after passing a maximum apex in $H_2/CO = 2$, activity decreases. It can be concluded that a low $H_2$/CO ratio leads to increased CO adsorption relative to hydrogen because it is well known that CO adsorption is stronger than the H on the catalyst [33, 34]. However, at a $H_2$/CO ratio of 2/1, the total selectivity toward $C_2$–$C_3$ olefins fraction was higher and the $CH_4$ selectivity was lower; in comparison with the products of the other $H_2$/CO feed ratios under the same operating conditions of temperature and pressure. Taking these results into consideration, the $H_2$/CO ratio of 2/1 was chosen as the optimum molar feed ratio for conversion of synthesis gas to $C_2$–$C_3$ light olefins fraction over the Co–Mn catalyst prepared by co-precipitation technique.

## Kinetic models (rate equations) for CO consumption and products

The production rate of each product and consumption rate of CO have been assumed to be a power-law form and also a function of the partial pressures of carbon monoxide and hydrogen as follows:

$$r_i = k_{i,0}\exp\left(\frac{-E_i}{RT}\right)P_{\mathrm{CO}}^{m_i}P_{\mathrm{H_2}}^{n_i}, \tag{8}$$

where $k_{i,0}$ and $E_i$ are the frequency factor and activation energy for the component $i$, respectively. To estimate the parameters of the kinetic model, the Levenberg–Marquardt (LM) algorithm still plays an important role. A non-linear regression algorithm of LM was utilized to fit the rival rate expressions to the experimental results by minimizing the summation of the squares of the deviations as follows and estimation of the reaction rate constants:

$$f_{i,\mathrm{obj}} = \sum_{i=1}^{N}\left(\frac{r_i^{\mathrm{exp}} - r_i^{\mathrm{cal}}}{r_i^{\mathrm{exp}}}\right)^2. \tag{9}$$

The $R^2$ value (reflects the amount of variance) and root mean square deviation (RMSD) of the involved rate measurement are reported as measures of the fit goodness:

$$\sigma = \frac{1}{N_{\mathrm{exp}}}\sum_{i=1}^{N_{\mathrm{exp}}} r_{\mathrm{CO},i}^{\mathrm{exp}} \tag{10}$$

$$R^2 = 1 - \left(\frac{\sum_{i=1}^{N_{\mathrm{exp}}}\left(r_{\mathrm{CO},i}^{\mathrm{exp}} - r_{\mathrm{CO},i}^{\mathrm{cal}}\right)^2}{\sum_{i=1}^{N_{\mathrm{exp}}}\left(r_{\mathrm{CO},i}^{\mathrm{exp}} - \sigma\right)^2}\right)^2 \tag{11}$$

and RMSD is described as

**Table 6** Kinetic models for the CO conversion rate and production rates of hydrocarbons

| $r_i = k_{i,0}\exp\left(\frac{-E_i}{RT}\right)P_{CO}^{m_i}P_{H_2}^{n_i}$ | | | | | | | | |
|---|---|---|---|---|---|---|---|---|
| $i$ | $k_{i,0}$ ($x$) (mmol $g^{-1}$ $min^{-1}$ $bar^x$) | $E_i$ (kJ/mol) | $m_i$ | $n_i$ | $R^2$ | RMSD | Variance | MARR (%) |
| CO | 102 (−1.58) | 30.71 | −0.38 | 1.96 | 0.94 | 0.018 | 0.014 | 19.21 |
| $CH_4$ | 202.99 (−1.04) | 42.37 | −0.88 | 1.92 | 0.94 | 1.88E−03 | 1.41E−04 | 20.87 |
| $C_2H_4$ | 84.69 (−1.02) | 34.53 | −0.33 | 1.35 | 0.94 | 5.11E−03 | 1.03E−03 | 13.73 |
| $C_3H_6$ | 102.01 (−1.19) | 30.58 | 0.64 | 0.55 | 0.96 | 4.53E−03 | 8.11E−04 | 13.22 |
| $C_4H_{10}$ | 0.31 (−1.33) | 17.49 | 0.78 | 0.55 | 0.95 | 3.05E−04 | 3.69E−06 | 11.86 |
| $C_5^+$ | 101.98 (−1.6) | 16.04 | −0.22 | 1.83 | 0.9 | 0.089 | 0.047 | 16.52 |

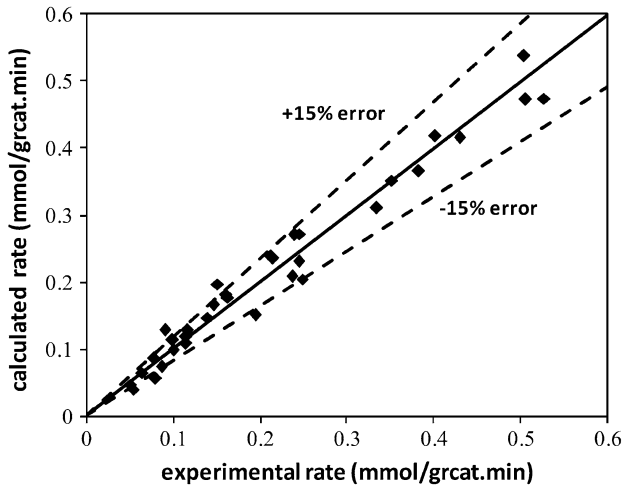


**Fig. 2** Parity plot of the propylene rate equation

$$\mathrm{RMSD} = \frac{1}{N_{\exp}}\left(\sum_{i=1}^{N_{\exp}}\left(r_{\mathrm{CO},i}^{\exp} - r_{\mathrm{CO},i}^{\mathrm{cal}}\right)^2\right)^2 \quad (12)$$

$r_{\mathrm{CO},i}^{\exp}$ and $r_{\mathrm{CO},i}^{\mathrm{cal}}$ indicate the experimental and calculated CO conversion rate from each kinetic model in the $i$th data point, respectively. $N_{\exp}$ represents the number of experimental data points with pure error variance $\sigma$.

The mean absolute relative residual (MARR) between experimental and calculated consumption rate of CO is defined as

$$\mathrm{MARR} = \frac{1}{N_{\exp}}\sum_{i=1}^{N_{\exp}}\left|\frac{r_i^{\exp} - r_i^{\mathrm{cal}}}{r_i^{\exp}}\right| \times 100. \quad (13)$$

The parameters obtained in the proposed expression for FT reaction and production rates of hydrocarbons in this study are shown in Table 6. The 95 % confidence intervals are much smaller than the parameter values. The high value of $R^2$ and low values of variance, RMSD and MARR, are obtained from these equations. Figure 2 shows a comparison between the experimental results and predicted kinetic model for the propylene production, as example. The solid line in the figure denotes that calculated $r_{C_3H_6}$ is equal to the experimental one and dotted lines over and under the solid line represent 15 % deviation. The experimental results were found a good agreement with the proposed kinetic model showing about 15 % deviation.

In comparison with other models, the power-law model can predict the effect of CO and $H_2$ concentration on reaction rate of production using $m$ and $n$ parameters. As can be seen in Table 6, the orders of reactions that were −0.38 and 1.96 for CO and $H_2$ are consistent with those reported in previous kinetic studies of FTS on cobalt-supported catalyst [19–23]. In all of those kinetic expressions, the coefficient $m$ was negative and the coefficient $n$ was positive, suggesting inhibition by adsorbed CO. The activation energy for the FT reaction obtained from power-law equation is 30.71 kJ/mol. In our previous research on the present catalyst [2], two kinetic expressions based on Langmuir–Hinshelwood–Hougen–Watson mechanism were observed to fit the experimental data accurately for FTS reaction. Activation energies were obtained to be 35.1 and 44.6 kJ/mol for optimal kinetics models. The activation energy is different for the two proposed models (power-law equation and optimal kinetics models). It may be due to the other coefficients which affect the activation energy of power law equation significantly.

The results show that the maximum activation energy and lower value of MARR have been for the methane and butane productions, respectively. Also, a rise in power of the partial pressure of CO from −0.88 to about 1 is observed which indicates that CO inhibits the production of hydrocarbons, i.e., methane, ethylene, and heavier hydrocarbons but this inhibiting tendency seems to diminish through propylene and butane.

## Conclusion

An active 25 %Co/75 %Mn/30 wt.% $TiO_2$ catalyst was prepared by co-precipitation method and it showed the highest performance for synthesis of light olefins in FTS. The optimal operating conditions for the production of light olefins were found to be 270 °C under the total pressure of 3 bar at the molar feed ratio of $H_2/CO = 2/1$.

The initial production rates and CO consumption rate were determined in a fixed-bed micro reactor by altering reaction temperature (190–270 °C), pressure (1–10 bar), GHSV (2,700–5,200 $h^{-1}$), and $H_2$/CO feed molar ratio (1–3). The results of the experiments are presented as power-law rate equations for FT reaction and each of the main products in Table 6. The unknown kinetic parameters were estimated from experimental data using nonlinear regression (Levenberg–Marquardt) method. The estimated model is comprehensive because it involves products like methane, ethylene, propylene, butane, and heavier hydrocarbons. It was observed that the model for the CO consumption shows an error of ±19 % while the models for the other hydrocarbons show a maximum error of ±21 %.



## References

1. Atashi H, Mansouri M, Hosseini SH, Khorram M, Mirzaei AA, Karimi M, Mansouri G (2012) Intrinsic kinetics of the Fischer–Tropsch synthesis over an impregnated cobalt–potassium catalyst. Korean J Chem Eng 29:304–309
2. Atashi H, Siami F, Mirzaei AA, Sarkari M (2010) Kinetic study of Fischer–Tropsch process on titania-supported cobalt–manganese catalyst. J Ind Eng Chem 16:952–961
3. Fischer F, Tropsch H (1923) Uber die Herstellung synthetischer olgemische (Synthol) durch Aufbau aus Kohlenoxyd und Wasserstoff. Brennst Chem 4:276–285
4. Kim YH, Hwang DY, Song SH, Lee SB, Park ED, Park MJ (2009) Kinetic parameter estimation of the Fischer–Tropsch synthesis reaction on K/Fe–Cu–Al catalysts. Korean J Chem Eng 26:1591–1600
5. Shen WJ, Zhou JL, Zhang BJ (1994) Kinetics of Fischer–Tropsch synthesis over precipitated iron catalyst. J Nat Gas Chem 4:385–400
6. Vannice MA (1975) The catalytic synthesis of hydrocarbons from $H_2$ CO mixtures over the group VIII metals: I. The specific activities and product distributions of supported metals. J Catal 37:449–461
7. Iglesia E (1997) Design, synthesis, and use of cobalt-based Fischer–Tropsch synthesis catalysts. Appl Catal A 161:59–78
8. Jeon JK, Kim CJ, Park YK, Ihm SK (2004) Catalytic properties of potassium-or lanthanum-promoted Co/γ–$Al_2O_3$ catalysts in carbon monoxide hydrogenation. Korean J Chem Eng 21:365–369
9. Khodakov AY, Chu W, Fongarland P (2007) Advances in the development of novel cobalt Fischer–Tropsch catalysts for synthesis of long-chain hydrocarbons and clean fuels. Chem Rev 107:1692–1744
10. Fan G, Zou B, Cheng S, Zheng L (2010) Ligandless palladium supported on SiO2–$TiO_2$ as effective catalyst for Suzuki reaction. J Ind Eng Chem 16:220–223
11. Brik Y, Kacimi M, Ziyad M, Bonzon-Verduraz F (2001) Titania-supported cobalt and cobalt–phosphorus catalysts: characterization and performances in ethane oxidative dehydrogenation. J Catal 202:118–128
12. Barrault J, Forguy C, Menezo J, Maurel R (1981) Hydrocondensation of $CO_2$ (CO) over supported iron catalysts. React Kinet Catal Lett 17:373–378
13. Barrault J, Forguy C, Perrichon V (1983) Effects of manganese oxide and sulphate on olefin selectivity of iron supported catalysts in the Fischer–Tropsch reaction. Appl Catal A 5:119–125
14. Mirzaei AA, Faizi M, Habibpour R (2006) Effect of preparation conditions on the catalytic performance of cobalt manganese oxide catalysts for conversion of synthesis gas to light olefins. Appl Catal A 306:98–107
15. Feyzi M, Khodaei MM, Shahmoradi J (2012) Effect of preparation and operation conditions on the catalytic performance of cobalt-based catalysts for light olefins production. Fuel Process Technol 93:90–98
16. Zare A, Zare A, Shiva M, Mirzaei AA (2013) Effect of calcination and reaction conditions on the catalytic performance of Co–Ni/$Al_2O_3$ catalyst for CO hydrogenation. J Ind Eng Chem 19:1858–1868
17. Wojciechowski BW (1988) The kinetics of the Fischer–Tropsch synthesis. Catal Rev Sci Eng 30:629–702
18. Botes FG, Dyk BV, McGregor C (2009) The development of a macro kinetic model for a commercial Co/Pt/$Al_2O_3$ Fischer–Tropsch catalyst. Ind Eng Chem Res 48:10439–10447
19. Zennaro R, Tagliabue M, Bartholomew CH (2000) Kinetics of Fischer–Tropsch synthesis on titania-supported cobalt. Catal Today 58:309–319
20. Wang J (1987) Physical, chemical, and catalytic properties of borided cobalt Fischer–Tropsch catalysts. Ph.D. thesis, Brigham Young University, Provo
21. Mansouri M, Atashi H, Setareshenas H (2013) Detailed kinetic study of the FTS over the co-precipitated Co-Ce/SiO2. Lambert Academic Publishing, Saarbrüchen
22. Yang CH, Massoth FE, Oblad AG (1979) Kinetics of CO + $H_2$ reaction over Co–Cu–$Al_2O_3$ catalyst. Adv Chem Ser 178:35–46
23. Brötz WZ (1949) Zur Systematik der Fischer–Tropsch-Katalyse. Zeitschrift für. Elektrochemie 5:301–306
24. Herington EFG (1946) The Fischer–Tropsch synthesis considered as a polymerization reaction. Chem Ind 65:346–347
25. Lox ES, Marin GB, de Graeve E, Bussiere P (1988) Characterization of a promoted precipitated iron catalyst for Fischer–Tropsch synthesis. Appl Catal A 40:197–218
26. Lox ES, Froment GF (1993) Kinetics of the Fischer–Tropsch reaction on a precipitated promoted iron catalyst. 1. Experimental procedure and results. Ind Eng Chem Res 32:61–70
27. Kim JS, Lee SM, Lee SB, Choi MJ, Lee KW (2006) Performance of catalytic reactors for the hydrogenation of $CO_2$ to hydrocarbons. Catal Today 115:228–234
28. Fernandes FAN (2005) Polymerization kinetics of Fischer–Tropsch reaction on iron based catalysts and product grade optimization. Chem Eng Tech 28:930–938
29. Gaube J, Herzog K, König L, Schliebs B (1986) Kinetische untersuchungen der Fischer–Tropsch-synthese zur klärung der wirkung des alkali als promotor in eisen-katalysatoren. Chem Ing Tech 58:682–683
30. Krishna KR, Bell AT (1993) Estimates of the rate coefficients for chain initiation, cropagation, and termination during Fischer–Tropsch synthesis over Ru/$TiO_2$. J Catal 139:104–118
31. Gribval-Constant A, Khodakov AY, Bechara R, Zholobenk VL (2002) Support mesoporosity: a tool for better control of catalytic behavior of cobalt supported Fischer–Tropsch catalysts. Stud Surf Sci Catal 144:609–616
32. Malek Abbaslou RM, Slotan Mohammadzadeh JS, Dalai AK (2009) Review on Fischer–Tropsch synthesis in supercritical media. Fuel Process Technol 90:849–856

33. Tian L, Huo CF, Cao DB, Yang Y, Xu J, Wu BS, Xiang HW, Xu YY, Li YW (2010) Effects of reaction conditions on iron-catalyzed Fischer–Tropsch synthesis: a kinetic Monte Carlo study. J Mol Struct Theochem 941:30–35

34. Christman K, Scober O, Neumann EGM (1974) Adsorption of CO on a Ni(111) surface. J Chem Phys 60:4719–4724